Title

Activity-Based Probe for N-Acylethanolamine Acid Amidase.

Journal

ACS Chemical Biology, 10(9)

Authors

Romeo, Elisa

Ponzano, Stefano

Armirotti, Andrea

et al.

Publication Date

2015-09-18

DOI

10.1021/acschembio.5b00197

Peer reviewed

HHS Public Access

Author manuscript

ACS Chem Biol. Author manuscript; available in PMC 2016 September 18.

Published in final edited form as:

ACS Chem Biol. 2015 September 18; 10(9): 2057–2064. doi:10.1021/acschembio.5b00197.

An Activity-Based Probe for N-Acylethanolamine Acid Amidase

Elisa Romeo[#†], **Stefano Ponzano**[#*,†], **Andrea Armirotti**[†], **Maria Summa**[†], **Fabio Bertozzi**[†], **Gianpiero Garau**[†], **Tiziano Bandiera**[†], and **Daniele Piomelli**[*,†,§]

[†]Drug Discovery and Development, Istituto Italiano di Tecnologia, Via Morego 30, I-16163 Genova, Italy

[§]Departments of Anatomy and Neurobiology, Pharmacology and Biological Chemistry, University of California, 3216 Gillespie Neuroscience Facility Irvine, California 92697-4621 (United States)

[#] These authors contributed equally to this work.

Abstract

N-Acylethanolamine acid amidase (NAAA) is a lysosomal cysteine hydrolase involved in the degradation of saturated and monounsaturated fatty acid ethanolamides (FAEs), a family of endogenous lipid signaling molecules that includes oleoylethanolamide (OEA) and palmitoylethanolamide (PEA). Among the reported NAAA inhibitors, α–amino–β–lactone (3–aminooxetan–2–one) derivatives have been shown to prevent FAE hydrolysis in innate-immune and neural cells and to reduce reactions to inflammatory stimuli. Recently, we disclosed two potent and selective NAAA inhibitors, the compounds ARN077 (5-phenylpentyl *N*-[(2*S*,3*R*)-2-methyl-4-oxo-oxetan-3-yl]carbamate) and ARN726 (4-cyclohexylbutyl-*N*-[(*S*)-2-oxoazetidin-3-yl]carbamate). The former is active in vivo by topical administration in rodent models of hyperalgesia and allodynia, while the latter exerts systemic anti-inflammatory effects in mouse models of lung inflammation. In the present study, we designed and validated a derivative of ARN726 as the first activity-based protein profiling (ABPP) probe for the in vivo detection of NAAA. The newly synthesized molecule **1** is an effective in vitro and in vivo click-chemistry activity based probe (ABP), which is able to capture the catalytically active form of NAAA in Human Embryonic Kidney 293 (HEK293) cells overexpressing human NAAA as well as in rat lung tissue. Competitive ABPP with **1** confirmed that ARN726 and ARN077 inhibit NAAA in vitro and in vivo. Compound **1** is a useful new tool to identify activated NAAA both in vitro and in vivo, and to investigate the physiological and pathological roles of this enzyme.

INTRODUCTION

N–acylethanolamine acid amidase (NAAA) is a cysteine hydrolase that belongs to the *N*-terminal nucleophile (Ntn) family of enzymes[1-3]. It is localized to lysosomes and bears a significant degree of sequence homology with the bacterial choloylglycine hydrolases, which are characterized by the ability to cleave non-peptide amide bonds.[4] Like other Ntn

[*]Corresponding author: S.P. stefano.ponzano@iit.it ; D.P. piomelli@uci.edu.

Supporting information

Supporting information includes Methods, Supplementary Figures S1 and S2, and Supplementary Tables S1-S3. This material is available free of charge via the Internet at http://pubs.acs.org.

enzymes, NAAA is activated by auto-proteolysis at acidic pH, which generates a catalytically competent form of the enzyme.[5] Site-directed mutagenesis experiments have unequivocally identified Cys131 (in mice) or Cys126 (in humans) as the amino acid residue responsible for both enzyme auto-proteolysis and catalytic activity.[6-8]

NAAA shares 33-34% identity with acid ceramidase (AC), another cysteine amidase found in lysosomes.[1] AC catalyzes the hydrolysis of medium-chain ceramides, which are important mediators of cell senescence and apoptosis,[9,10] and the formation of sphingosine, while NAAA is involved in the deactivating hydrolysis of fatty acid ethanolamides (FAEs), a class of lipid mediators that play important roles in the control of pain, inflammation and energy balance.[11,12] In particular, NAAA preferentially hydrolyzes monounsaturated and saturated FAEs, such as oleoylethanolamide (OEA, 18:1Δ)[9] and palmitoylethanolamide (PEA, 16:0),[1,2,13] over polyunsaturated FAEs like arachidonylethanolamide (anandamide, 20:4 Δ),[5,8,11,14] which is preferentially inactivated by fatty acid amide hydrolase (FAAH).[14,15] Anandamide is an endogenous agonist for cannabinoid receptors, and participates in the control of stress-coping responses and pain initiation,[16] among other functions, while PEA and OEA regulate pain, inflammation and energy balance primarily by ligating peroxisome proliferator-activated receptor-α (PPAR-α), a member of the nuclear receptor superfamily.[11,17-19]

The pharmacology of PEA has been extensively investigated.[12] The compound inhibits peripheral inflammation and mast cell degranulation,[20,21] and exerts profound anti-nociceptive effects in rat and mouse models of acute and chronic pain.[11,21-23] Moreover, in mice, PEA suppresses pain behaviors induced by tissue injury, nerve damage or inflammation.[18] These effects are dependent on PPAR-α activation, since they are absent in PPAR-α-null mice, blocked by PPAR-α antagonists, and mimicked by PPAR-α agonists.[18,24]

A limited number of natural[25] or synthetic[26-31] NAAA inhibitors have been reported thus far. Among them, α–amino–β–lactone (3–aminooxetan–2–one) derivatives have shown promise because of their high inhibitory potency and target selectivity.[32-36]

In vitro and in vivo studies have demonstrated that this class of compounds blocks PEA and OEA hydrolysis in host-defense cells, such as macrophages and sensory neurons, and dampens tissue reactions to various inflammatory stimuli.[34,35] For example topical administration of 5–phenylpentyl *N*-[(2*S*,3*R*)-2-methyl-4-oxo-oxetan-3-yl]carbamate (ARN077, Figure 1),[32,33] a potent and selective β-lactone NAAA inhibitor [rat NAAA (rNAAA) median inhibitory concentration, IC_{50} = 50 nM, human NAAA (hNAAA) IC_{50} = 7 nM], elevates PEA and OEA levels in mouse skin and sciatic nerve, and attenuates nociception in mice and rats.[37] Nevertheless, due to the inherent instability of β-lactone compounds, a program aimed at the identification of novel NAAA inhibitors suitable for systemic administration was undertaken. This program led to the discovery of 3-aminoazetidin-2-ones derivatives as potentially useful NAAA-interacting probes.[38] Within this class, ARN726 (4-cyclohexylbutyl-*N*-[(*S*)-2-oxoazetidin-3-yl]carbamate) (Figure 1) emerged as a potent, selective and systemically active NAAA inhibitor (rNAAA IC_{50} = 63 nM, hNAAA IC_{50} = 27 nM).[39] In vivo experiments showed that systemic ARN726 exerts

pronounced anti-inflammatory effects in mouse models of carrageenan- and LPS-induced inflammation, and suppresses inflammatory reactions in human macrophages ex vivo.[39] These effects are ascribable to PPAR-α activation by endogenous PEA and OEA, the levels of which are increased after treatment with the inhibitor.[39]

High-resolution liquid chromatography–tandem mass spectrometry (LC–MS) analysis enabled us to elucidate the mechanism through which β-lactone and β-lactam derivatives inhibit NAAA activity. We showed that ARN077 and ARN726 block NAAA via formation of a thioester bond with its catalytic cysteine.[39,40] This result, together with the systemic activity demonstrated by ARN726,[39] prompted us to design an Activity-Based Protein Profiling (ABPP) probe that might be used to detect catalytically active NAAA in live animals. Similar β-lactams have been used as ABPP probes in bacterial proteomes to identify penicillin-binding proteins and other relevant targets.[41,42] Here, we describe a novel β-lactam ABPP probe for NAAA and utilize click chemistry-ABPP (CC-ABPP) methodology[43,44] to elucidate the in vitro and in vivo labeling profile of this compound.

The CC-ABPP technique (Figure 2) contemplates the use of a chemical probe with a terminal alkyne functionality, which is first incubated with intact cells or cell extracts and subsequently modified by 1,3-dipolar Huisgen cycloaddition[45-48] to introduce a reporter tag (e.g. biotin or rhodamine). Reacted proteins bearing the reporter tag can be subsequently identified by in-gel fluorescence detection, western blot and/or LC–MS analysis (Figure 2). This two-step method allows for a more efficient labeling of reactive proteins compared to the original ABPP procedure, where the reporter tagged probes usually show low cell permeability and lower selectivity towards target enzymes.[41,43]

RESULTS AND DISCUSSION

The design of the ABPP probe **1** (ARN14686, undec-10-ynyl *N*-[(3*S*)-2-oxoazetidin-3-yl]carbamate) was based on the chemical structure of the systemically active NAAA inhibitor ARN726 (Figure 1).[39] We did not modify the azetidin-2-one ring of ARN726, which reacts with the catalytic cysteine of NAAA, but replaced the 4-butyl-cyclohexyl group with a C9 saturated aliphatic chain bearing a terminal alkyne tag (Figure 2a). We selected a C9 chain for two reasons: first, previous work had shown that NAAA displays higher affinity for inhibitors with long aliphatic chains[33,38] and, second, we expected that such a chain would facilitate the interaction between the alkyne moiety of **1** and the azide group of the reporter tag during the click chemistry reaction. The chemical synthesis of **1** is described under Supporting Information.

We examined the ability of **1** to inhibit NAAA activity by assessing the hydrolysis of *N*-(4-methyl-2-oxo-chromen-7-yl)-hexadecanamide (PAMCA) using recombinant hNAAA heterologously expressed in HEK293 cells (see Supporting Information). Compound **1** inhibited hNAAA with high potency (IC_{50} = 0.006 μM; compared to IC_{50} = 0.073 μM for ARN726). The compound also inhibited rNAAA (IC_{50} = 0.013 μM), while having only a weak inhibitory effect on rat AC (IC_{50} = 1.2 μM). As previously shown for ARN726,[39] compound **1** interacts with NAAA via covalent binding to the *N*-terminal cysteine. High-resolution LC–MS analyses showed that probe **1**, upon incubation at acidic pH (4.5) with

active purified hNAAA, forms a covalent adduct with the *N*-terminal peptide of the enzyme through *S*-acylation of its catalytic cysteine. Figure 3a reports the full MS/MS spectrum of hNAAA N-terminus peptide CTSIVAQDSR acylated by **1**. Labeling occurs on the cysteine residue (see *b* fragment ion series reported in Figure 3b) and two side-chain fragments are consistent with the formation of a thioester adduct (Figure 3c).

To evaluate the usefulness of **1** as a click chemistry probe, we incubated the compound with purified hNAAA (which was preventively activated at acidic pH), coupled an azide-PEG3-biotin conjugate to its terminal alkyne using click chemistry,[49] and visualized protein bands using streptavidin-horseradish peroxidase (HRP). The labeling step was performed either in phosphate buffered saline (PBS, pH 7.4) or in phosphate/ citrate buffer, pH 4.5, while in both cases PBS was used as buffer for the click chemistry reaction. As shown in Figure 4a, a chemiluminescent signal was visible at the apparent molecular mass of catalytically active NAAA β–subunit, and no differences were observed at the two chosen pH. By contrast, both active enzyme and full-length inactive protein were detected when using an anti-NAAA antibody. This result indicates that **1** binds only to the catalytically active form of NAAA, and may serve therefore as an efficient activity-based probe. The interaction of **1** with NAAA was further evaluated using different concentrations of the probe with fixed amounts of purified hNAAA, or vice versa. As shown in Figure 4b, when increasing concentrations of **1** (from 0.01 μM to 10 μM) were incubated with a fixed amount of purified hNAAA (1μM), a proportional increase in chemiluminescent signal was noted. A similar result was obtained when changing the protein amount while keeping the probe concentration constant (10 μM) (Figure 4c). We performed this experiment in the presence of a background proteome (10 μg of HEK293 cell extract). As shown in Figure 4c, the lowest concentration of NAAA detected by the probe was 1,25 pmoles.

We further validated **1** by testing the ability of the probe to label intact HEK293 cells that overexpress hNAAA (NAAA-HEK293). As shown in Figure 5a, incubations of intact cells or cell lysates with **1** yielded results similar to those obtained with purified enzyme, and only bands associated with the activated β-subunit of NAAA were tagged by streptavidin-HRP. When the anti-NAAA antibody was applied to blot membranes both intact and cleaved NAAA were detected, with a prevalence of the activated form of the enzyme. This experiment highlights the high versatility of **1**, which can be efficiently used to detect NAAA both in cell lysates and in intact cells were the labeling occurs inside the lysosomes. In a similar experiment (Figure 5b), we preincubated NAAA-HEK293 cells with ARN726 (lane 3) or ARN077 (lane 4) and then added an equimolar concentration of **1**. In either case, a decrease in signal intensity was observed, but a more pronounced masking of NAAA was noted with ARN726 than with ARN077. This is consistent with the partial reversibility of ARN077 observed in dialysis experiments[40] and with our findings that the covalent adduct formed by β-lactones with NAAA undergoes hydrolysis under the conditions of the assay, whereas the covalent adduct formed by β-lactams does not (unpublished data).

To check whether the signal of the band associated with overexpressed NAAA could partially or completely mask other unwanted targets, we repeated the experiment using wild type (wt) HEK293 cells, which do not constitutively express NAAA (Supplementary Figure S1). The cells were incubated in the presence of **1** and then cytosol and membrane fractions

were isolated. The entire CC-ABPP protocol was carried out, including the enrichment phase on streptavidin beads and LC–MS analysis of the enriched proteome. As a positive control, we used a maleimide-containing probe (**2**, see Supporting Information), incubated it with wt HEK293 cells and applied the CC-ABPP procedure to cytosol and membrane fractions. As shown in Figure 6a, in wt HEK293 incubated with **1**, no significant bands were detected by protein blot. Conversely, when the same cells were incubated with **2**, intense chemiluminescent signals were observed throughout the range of molecular masses, indicating that HEK293 cells express a large number of proteins that could potentially react with an electrophilic probe such as **1**. The total lysate of NAAA-HEK293 incubated with **1** was also used as a control (lane 5, Figure 6a). To further evaluate the possible presence of off-targets of **1**, the same sample from HEK293 or NAAA-HEK293 incubated with **1** was enriched using streptavidin-agarose and the eluted proteins were analyzed by protein blot. As shown in Figure 5b, no spurious target could be detected in HEK293 cells, even after the enrichment phase, whereas NAAA was clearly identified in HEK293 cells overexpressing the enzyme.

As last step to ensure the identification of all possible targets of **1**, the streptavidin enriched proteins of HEK293 and NAAA-HEK293 were also analyzed by LC–MS/MS. The findings confirmed that NAAA was the only labeled enzyme in NAAA-HEK293 cells (Supplementary Table S1).

The ability of **1** to label NAAA in intact cells encouraged us to examine the efficiency and selectivity of the probe under more challenging experimental conditions, such as those offered by in vivo treatments and analysis of homogenates and tissue fractions prepared from freshly dissected organs. We examined therefore whether **1** was able to label NAAA in rat lungs, which are known to contain the enzyme in relatively high levels.[2] We first prepared various tissue fractions (total lysate, membrane, cytosol and lysosome fractions) and incubated them with two different concentrations of **1** (1 and 10 μM). We performed the CC-ABPP protocol, including the streptavidin enrichment phase, and analyzed the labeled proteins by protein blot as shown in Figure 7a. Consistent with our previous findings, a protein band with the apparent molecular mass of NAAA was visualized in the lysosomal fraction incubated with the two different concentrations of **1** (1 or 10 μM). At the highest concentration used, another weaker signal with apparent molecular mass of 37 kDa was observed. Moreover, a protein band at around 68 kDa was detected in the total lysate and the cytosolic fraction. LC–MS analyses of the streptavidin-enriched proteins confirmed the presence of rNAAA in the lysosome fraction and identified the 37 KDa band as AC, while the 68 kDa protein corresponded to serum albumin. These additional targets were present only in samples exposed to the highest concentration of **1**, which at 1 μM was highly selective for NAAA (Supplementary Table S2). The expression of NAAA and AC in the rat lung cellular fractions was analyzed also by western blot using specific antibodies (Supplementary Figure S2).

Finally, we investigated the ability of **1** to act as a selective activity-based probe for NAAA in vivo. We administered the compound by intravenous (i.v.) injection (10 mg/kg) in either naïve rats or rats that were pretreated with ARN726 (10 mg/kg, i.v.). Lysosomal lung preparations were used for click chemistry and streptavidin enrichment. The protein blot

results illustrated in Figure 7b indicate that ARN726 competed with **1** for binding to both NAAA and AC (lane 3, Figure 7b). The binding of ARN726 and **1** to AC is not unexpected, given the high exposure achieved with the 10 mg/kg i.v. dose of the two compounds. In agreement with previous results, when rats were treated only with **1** the bands associated to NAAA and AC (lane 4, Figure 7b) were clearly visible. The presence of NAAA and AC as the only targets of **1** was confirmed by LC–MS analysis of the enriched proteome (Supplementary Table S3).

In conclusion, based on the scaffold of the serine-derived β-lactam ARN726, we designed and validated compound **1** as the first activity-based probe for NAAA. β-lactones and β-lactams are known to react with enzymes bearing active site nucleophiles and, thanks to the covalent nature of their inhibition and their customizable reactivity, they may be especially suitable for the design of activity-based probes.[41] Since mammals express a substantial number of proteins that could be potentially targeted by β-lactone and β-lactam probes, selectivity is an important issue. In this study, we provide evidence that **1** efficiently binds to the catalytically active form of NAAA and displays very high target selectivity both in vitro and in vivo. Among hundreds of known serine and cysteine proteases,[50] **1** interacted only with NAAA, indicating that it may offer a useful tool to identify activated NAAA in animal models and other complex biological systems. The recent finding that NAAA may be involved in tumor aggressiveness[51] highlights the relevance of this result. Moreover, we showed that, when administered at high concentrations/doses (10 μM in vitro, 10 mg/kg in vivo), **1** is able to bind AC, a key enzyme of sphingolipid metabolism that shares 33-34% identity and 70% similarity with NAAA. Uracil derivatives have been recently disclosed, which may be useful as ABPP probes for AC.[52] Our results suggest that the β-lactam scaffold may offer an additional starting point for the development of activity-based probes for AC and, possibly, other cysteine hydrolases.

METHODS

Sample preparation for CC-ABPP analysis on purified hNAAA

Purified hNAAA (2 μM) was incubated in activation buffer [100mM Sodium Phosphate Buffer, 100 mM Sodium Citrate, 3mM TCEP, 0.1% Triton ×100, pH4.5] for 2h at 37 °C. The labeling with compound **1** (20 μM, for 1.5 h at 37 °C) was performed either in activation buffer (pH 4.5) or in PBS (pH 7.4) following a buffer exchange step using desalting columns. After incubation with the probe, the buffer of both samples was exchanged with PBS and the click chemistry reaction was performed. Control samples containing DMSO were also prepared. For the concentration-response curves, the amount of NAAA and **1** were as indicated in Figure 4, and the labeling pH was pH7.4. To determine the detection limit of NAAA by **1** (Figure 4c), the purified protein (5 μg) was dissolved in 100 μl of wt HEK293 protein extract (1 mg/ml, in PBS buffer) and then 1 to 2 serial dilutions in HEK293 proteome (1 mg/ml) were prepared. Protein samples were subjected to click chemistry for biotin addition, as described below, and samples (10 μl) were analyzed by gel-electrophoresis and protein blot.

Sample preparation for CC-ABPP analysis on cell lines

For the in vitro CC-ABPP on cell lysates, NAAA-overexpressing HEK293 cells (1×10^7) were lysed by sonication (Sonopuls HD 2200, Bandelin, D) in 4 volumes of PBS/Sucrose 0.32 M at pH 7.4 and protease inhibitor cocktail (Sigma-Aldrich product #P8340). The suspension was centrifuged at 800×g for 20 min at 4°C to discard nuclei and cell debris. The total extracted proteins were quantified with BCA protein assay (Euroclone). The protein extracts were diluted to 2 mg/ml (500 μl) and incubated with **1** (10 μM) or DMSO only, for 1 h at 37°C. Click chemistry was performed as described below. For the in-cells CC-ABPP, cells (wild type HE293 or hNAAA overexpressing HEK293) were cultured in suspension with FreeStyle 293 expression medium (Life Technologies) and treated with **1** or **2** (40 μM) for 1h at 37°C. For competitive ABPP, cells were first incubated with ARN726 (40 μM) or ARN077 (40 μM) and then **1** (40 μM) was added. For each experiment, cells treated with DMSO were used as control. After treatment, cells were lysed in PBS/0.32 M sucrose pH 7.4 as described above. For the analysis of total cell proteome, the suspension was centrifuged for 20 min at 800×g at 4°C and the supernatant was saved (total lysate). For the experiments on cell fractions, the supernatant was centrifuged at 100,000×g to obtain total cell membranes (pellet) and cytosol (supernatant). For each sample, extracted proteins were quantified using the BCA assay (Euroclone). The samples were stored at −80°C until use. The click chemistry reaction was performed as described below.

Animals

We used male Sprague-Dawley rats, weighing 175–200 g (Charles River). All procedures were performed in accordance with the Ethical Guidelines of European Communities Council (Directive 2010/63/EU of 22 September 2010) and accepted by the Italian Ministry of Health. All efforts were made to minimize animal suffering and to use the minimal number of animals required to produce reliable results. Animals were group-housed in ventilated cages and had free access to food and water. They were maintained under a 12-hour light/dark cycle (lights on at 8:00 am) at controlled temperature (21°C ± 1°C) and relative humidity (55% ± 10%). Experimenters were unaware of the treatment protocol at the time of the test (blind procedure).

Sample preparation for CC-ABPP analysis on rat lungs

Three rats per dose were used. **1** or ARN726 were dissolved in PEG400/Tween 80/Saline solution at 10/10/80% in volume respectively and administered intravenously (i.v.) at the dose of 10 mg kg^{-1}. For the competition assay, rats were pretreated with ARN726 for 1 h and then **1** was administered for one additional h. After treatments, the rats were sacrificed and lungs were immediately dissected, frozen on dry ice, and stored at −80°C until analyses. Lungs were homogenized in PBS pH 7.4/0.32M sucrose using an IKA T-18 Ultraturrax homogenizer. Samples were then centrifuged 25min at 800×g. The supernatant was centrifuged for 30 min at 12,000×g at 4°C. The pellets were suspended in 2 volumes of PBS and subjected to two freeze/thaw cycles at −80°C to solubilize proteins. The suspensions were centrifuged at 105,000×g for 1 h at 4°C and the soluble fraction was taken. For the in vitro experiments, lungs were obtained from naïve rats (without treatment) and homogenized as described above. The supernatant obtained after the first centrifugation at

800×g (total lysate) was centrifuged again either at 105,000×g to obtain total membranes (pellet fraction) and cytosol (soluble fraction) or at 12,000×g as described above for the in vivo experiments. The membranes were suspended in 4 volumes of PBS. Protein concentration was measured by BCA assay (Euroclone) and samples were stored at −80°C until use. The probe was added at 10 μM for 1 h at 37°C. The click chemistry reaction was performed as described below.

Click chemistry and streptavidin enrichment

The click chemistry and the streptavidin enrichment were performed according to the protocol described in Speers A. E. et al. 2009.[49] Briefly, the following reagents were added to the protein preparations at the indicated final concentration: 100μM Azide-PEG3-biotin conjugate (CLK-AZ104P4, Jena Bioscience), 1mM TCEP, 100 μM Tris[(1-benzyl-1H-1,2,3-triazol-4-yl)methyl]amine (TBTA), 1mM CuSO4.5H2O. TBTA was first dissolved in DMSO at 83.5mM and then diluted with four volumes of t-butanol. The reaction was mixed by vortexing and incubated 1h at 25°C. The volumes of reaction were 2× 500μl (1mg/ml protein concentration) when streptavidin enrichment was required, and 50μl (1mg/ml protein concentration) when only protein blot analysis was performed. After the reaction time the samples were either directly analyzed by protein blot or streptavidin enriched as described.[49] Briefly, the proteins were first extracted by methanol/chloroform extraction, the final protein pellet was suspended in 650μl of SDS 2.5 % and sonicated 3×10sec, heated at 65°C per 5 min and sonicated again. Finally, the samples were centrifuged to remove the possible insolubilized fraction. The percentage of SDS was diluted to 0.2% by PBS addition and 100μl of streptavidin-agarose resin (50% slurry, product #20353, Thermo Scientific) were added 1h at RT. The streptavidin beads were collected by centrifugation and washed with 1% SDS, 6M urea, and PBS. The recovered beads were treated accordingly to the further application.

Supplementary Material

Refer to Web version on PubMed Central for supplementary material.

Acknowledgements

We thank G. Ottonello, S. Mandrup-Bertozzi, L. Mengatto, and L. Goldoni for experimental help. We thank A. Fiasella and A. Nuzzi for kindly providing ARN726. This work was partially supported by the National Institute on Drug Abuse (to DP).

REFERENCES

(1). Tsuboi K, Sun YX, Okamoto Y, Araki N, Tonai T, Ueda N. Molecular characterization of N-acylethanolamine-hydrolyzing acid amidase, a novel member of the choloylglycine hydrolase family with structural and functional similarity to acid ceramidase. J. Biol. Chem. 2005; 280:11082–11092. [PubMed: 15655246]

(2). Tsuboi K, Takezaki N, Ueda N. The N-acylethanolamine-hydrolyzing acid amidase (NAAA). Chem. Biodivers. 2007; 4:1914–1925. [PubMed: 17712833]

(3). Ueda N, Tsuboi K, Uyama T. N-acylethanolamine metabolism with special reference to N-acylethanolamine-hydrolyzing acid amidase (NAAA). Prog. Lipid. Res. 2010; 49:299–315. [PubMed: 20152858]

(4). Rossocha M, Schultz-Heienbrok R, von Moeller H, Coleman JP, Saenger W. Conjugated bile acid hydrolase is a tetrameric N-terminal thiol hydrolase with specific recognition of its cholyl but not of its tauryl product. Biochemistry. 2005; 44:5739–5748. [PubMed: 15823032]

(5). Zhao LY, Tsuboi K, Okamoto Y, Nagahata S, Ueda N. Proteolytic activation and glycosylation of N-acylethanolamine-hydrolyzing acid amidase, a lysosomal enzyme involved in the endocannabinoid metabolism. Biochim. Biophys. Acta. 2007; 1771:1397–1405. [PubMed: 17980170]

(6). Wang J, Zhao LY, Uyama T, Tsuboi K, Tonai T, Ueda N. Amino acid residues crucial in pH regulation and proteolytic activation of N-acylethanolamine-hydrolyzing acid amidase. Biochim. Biophys. Acta. 2008; 1781:710–717. [PubMed: 18793752]

(7). West JM, Zvonok N, Whitten KM, Vadivel SK, Bowman AL, Makriyannis A. Biochemical and mass spectrometric characterization of human N-acylethanolamine-hydrolyzing acid amidase inhibition. PLoS One. 2012; 7:e43877. [PubMed: 22952796]

(8). West JM, Zvonok N, Whitten KM, Wood JT, Makriyannis A. Mass spectrometric characterization of human N-acylethanolamine-hydrolyzing acid amidase. J. Proteome Res. 2012; 11:972–981. [PubMed: 22040171]

(9). Hannun YA, Obeid LM. Principles of bioactive lipid signalling: lessons from sphingolipids. Nat. Rev. Mol. Cell. Biol. 2008; 9:139–150. [PubMed: 18216770]

(10). Kitatani K, Idkowiak-Baldys J, Hannun YA. The sphingolipid salvage pathway in ceramide metabolism and signaling. Cell. Signal. 2008; 20:1010–1018. [PubMed: 18191382]

(11). Calignano A, La Rana G, Giuffrida A, Piomelli D. Control of pain initiation by endogenous cannabinoids. Nature. 1998; 394:277–281. [PubMed: 9685157]

(12). LoVerme J, La Rana G, Russo R, Calignano A, Piomelli D. The search for the palmitoylethanolamide receptor. Life Sci. 2005; 77:1685–1698. [PubMed: 15963531]

(13). Ueda N, Yamanaka K, Yamamoto S. Purification and characterization of an acid amidase selective for N-palmitoylethanolamine, a putative endogenous anti-inflammatory substance. J. Biol. Chem. 2001; 276:35552–35557. [PubMed: 11463796]

(14). Cravatt BF, Giang DK, Mayfield SP, Boger DL, Lerner RA, Gilula NB. Molecular characterization of an enzyme that degrades neuromodulatory fatty-acid amides. Nature. 1996; 384:83–87. [PubMed: 8900284]

(15). Desarnaud F, Cadas H, Piomelli D. Anandamide amidohydrolase activity in rat brain microsomes. Identification and partial characterization. J. Biol. Chem. 1995; 270:6030–6035. [PubMed: 7890734]

(16). Piomelli D, Giuffrida A, Calignano A, Rodriguez de Fonseca F. The endocannabinoid system as a target for therapeutic drugs. Trends. Pharmacol. Sci. 2000; 21:218–224. [PubMed: 10838609]

(17). Fu J, Gaetani S, Oveisi F, Lo Verme J, Serrano A, Rodriguez De Fonseca F, Rosengarth A, Luecke H, Di Giacomo B, Tarzia G, Piomelli D. Oleylethanolamide regulates feeding and body weight through activation of the nuclear receptor PPAR-alpha. Nature. 2003; 425:90–93. [PubMed: 12955147]

(18). LoVerme J, Russo R, La Rana G, Fu J, Farthing J, Mattace-Raso G, Meli R, Hohmann A, Calignano A, Piomelli D. Rapid broad-spectrum analgesia through activation of peroxisome proliferator-activated receptor-alpha. J. Pharmacol. Exp. Ther. 2006; 319:1051–1061. [PubMed: 16997973]

(19). Schwartz GJ, Fu J, Astarita G, Li X, Gaetani S, Campolongo P, Cuomo V, Piomelli D. The lipid messenger OEA links dietary fat intake to satiety. Cell. Metab. 2008; 8:281–288. [PubMed: 18840358]

(20). Berdyshev E, Boichot E, Corbel M, Germain N, Lagente V. Effects of cannabinoid receptor ligands on LPS-induced pulmonary inflammation in mice. Life Sci. 1998; 63:PL125–129. [PubMed: 9718090]

(21). D'Agostino G, La Rana G, Russo R, Sasso O, Iacono A, Esposito E, Raso GM, Cuzzocrea S, Lo Verme J, Piomelli D, Meli R, Calignano A. Acute intracerebroventricular administration of palmitoylethanolamide, an endogenous peroxisome proliferator-activated receptor-alpha agonist, modulates carrageenan-induced paw edema in mice. J. Pharmacol. Exp. Ther. 2007; 322:1137–1143. [PubMed: 17565008]

(22). Calignano A, La Rana G, Piomelli D. Antinociceptive activity of the endogenous fatty acid amide, palmitylethanolamide. Eur. J. Pharmacol. 2001; 419:191–198. [PubMed: 11426841]

(23). Mazzari S, Canella R, Petrelli L, Marcolongo G, Leon A. N-(2-hydroxyethyl)hexadecanamide is orally active in reducing edema formation and inflammatory hyperalgesia by down-modulating mast cell activation. Eur. J. Pharmacol. 1996; 300:227–236. [PubMed: 8739213]

(24). Khasabova IA, Xiong Y, Coicou LG, Piomelli D, Seybold V. Peroxisome proliferator-activated receptor alpha mediates acute effects of palmitoylethanolamide on sensory neurons. J. Neurosci. 2012; 32:12735–12743. [PubMed: 22972997]

(25). De Petrocellis L, Ligresti A, Moriello AS, Allara M, Bisogno T, Petrosino S, Stott CG, Di Marzo V. Effects of cannabinoids and cannabinoid-enriched Cannabis extracts on TRP channels and endocannabinoid metabolic enzymes. Br. J. Pharmacol. 2011; 163:1479–1494. [PubMed: 21175579]

(26). Saturnino C, Petrosino S, Ligresti A, Palladino C, De Martino G, Bisogno T, Di Marzo V. Synthesis and biological evaluation of new potential inhibitors of N acylethanolamine hydrolyzing acid amidase. Bioorg. Med. Chem. Lett. 2010; 20:1210–1213. [PubMed: 20022504]

(27). Tsuboi K, Hilligsmann C, Vandevoorde S, Lambert DM, Ueda N. N-cyclohexanecarbonylpentadecylamine: a selective inhibitor of the acid amidase hydrolysing N-acylethanolamines, as a tool to distinguish acid amidase from fatty acid amide hydrolase. Biochem. J. 2004; 379:99–106. [PubMed: 14686878]

(28). Vandevoorde S, Tsuboi K, Ueda N, Jonsson KO, Fowler CJ, Lambert DM. Esters, retroesters, and a retroamide of palmitic acid: pool for the first selective inhibitors of N-palmitoylethanolamine-selective acid amidase. J. Med. Chem. 2003; 46:4373–4376. [PubMed: 14521402]

(29). Yamano Y, Tsuboi K, Hozaki Y, Takahashi K, Jin XH, Ueda N, Wada A. Lipophilic amines as potent inhibitors of N-acylethanolamine-hydrolyzing acid amidase. Bioorg. Med. Chem. 2012; 20:3658–3665. [PubMed: 22542283]

(30). Li Y, Yang L, Chen L, Zhu C, Huang R, Zheng X, Qiu Y, Fu J. Design and synthesis of potent N-acylethanolamine-hydrolyzing acid amidase (NAAA) inhibitor as anti-inflammatory compounds. PLoS One. 2012; 7:e43023. [PubMed: 22916199]

(31). Bandiera T, Ponzano S, Piomelli D. Advances in the discovery of N-acylethanolamine acid amidase inhibitors. Pharmacol. Res. 2014:11–17. [PubMed: 24798679]

(32). Duranti A, Tontini A, Antonietti F, Vacondio F, Fioni A, Silva C, Lodola A, Rivara S, Solorzano C, Piomelli D, Tarzia G, Mor M. N-(2-Oxo-3-oxetanyl)carbamic Acid Esters as N-Acylethanolamine Acid Amidase Inhibitors: Synthesis and Structure-Activity and Structure-Property Relationships. J. Med. Chem. 2012; 55:4824–4836. [PubMed: 22515328]

(33). Ponzano S, Bertozzi F, Mengatto L, Dionisi M, Armirotti A, Romeo E, Berteotti A, Fiorelli C, Tarozzo G, Reggiani A, Duranti A, Tarzia G, Mor M, Cavalli A, Piomelli D, Bandiera T. Synthesis and structure-activity relationship (SAR) of 2-methyl-4-oxo-3-oxetanylcarbamic acid esters, a class of potent N-acylethanolamine acid amidase (NAAA) inhibitors. J. Med. Chem. 2013; 56:6917–6934. [PubMed: 23991897]

(34). Solorzano C, Antonietti F, Duranti A, Tontini A, Rivara S, Lodola A, Vacondio F, Tarzia G, Piomelli D, Mor M. Synthesis and structure-activity relationships of N-(2-oxo-3-oxetanyl)amides as N-acylethanolamine-hydrolyzing acid amidase inhibitors. J. Med. Chem. 2010; 53:5770–5781. [PubMed: 20604568]

(35). Solorzano C, Zhu C, Battista N, Astarita G, Lodola A, Rivara S, Mor M, Russo R, Maccarrone M, Antonietti F, Duranti A, Tontini A, Cuzzocrea S, Tarzia G, Piomelli D. Selective N-acylethanolamine-hydrolyzing acid amidase inhibition reveals a key role for endogenous palmitoylethanolamide in inflammation. Proc. Natl. Acad. Sci. U.S.A. 2009; 106:20966–20971. [PubMed: 19926854]

(36). Vitale R, Ottonello G, Petracca R, Bertozzi SM, Ponzano S, Armirotti A, Berteotti A, Dionisi M, Cavalli A, Piomelli D, Bandiera T, Bertozzi F. Synthesis, structure-activity, and structure-stability relationships of 2-substituted-N-(4-oxo-3-oxetanyl) N-acylethanolamine acid amidase (NAAA) inhibitors. ChemMedChem. 2014; 9:323–336. [PubMed: 24403170]

(37). Sasso O, Moreno-Sanz G, Martucci C, Realini N, Dionisi M, Mengatto L, Duranti A, Tarozzo G, Tarzia G, Mor M, Bertorelli R, Reggiani A, Piomelli D. Antinociceptive effects of the N-

acylethanolamine acid amidase inhibitor ARN077 in rodent pain models. Pain. 2013; 154:350–360. [PubMed: 23218523]

(38). Fiasella A, Nuzzi A, Summa M, Armirotti A, Tarozzo G, Tarzia G, Mor M, Bertozzi F, Bandiera T, Piomelli D. 3-Aminoazetidin-2-one derivatives as N-acylethanolamine acid amidase (NAAA) inhibitors suitable for systemic administration. ChemMedChem. 2014; 9:1602–1614. [PubMed: 24828120]

(39). Ribeiro A, Pontis S, Mengatto L, Armirotti A, Chiurchiu V, Capurro V, Fiasella A, Nuzzi A, Romeo E, Moreno-Sanz G, Maccarrone M, Reggiani A, Tarzia G, Mor M, Bertozzi F, Bandiera T, Piomelli D. A Potent Systemically Active N-Acylethanolamine Acid Amidase Inhibitor that Suppresses Inflammation and Human Macrophage Activation. ACS Chem. Biol. 2015 DOI 10.1021/acschembio.1025b00114.

(40). Armirotti A, Romeo E, Ponzano S, Mengatto L, Dionisi M, Karacsonyi C, Bertozzi F, Garau G, Tarozzo G, Reggiani A, Bandiera T, Tarzia G, Mor M, Piomelli D. beta-Lactones Inhibit N-acylethanolamine Acid Amidase by S-Acylation of the Catalytic N-Terminal Cysteine. Acs Med. Chem. Lett. 2012; 3:422–426. [PubMed: 24900487]

(41). Bottcher T, Sieber SA. beta-Lactams and beta-lactones as activity-based probes in chemical biology. MedChemComm. 2012; 3:408–417.

(42). Staub I, Sieber SA. beta-lactams as selective chemical probes for the in vivo labeling of bacterial enzymes involved in cell wall biosynthesis, antibiotic resistance, and virulence. J. Am. Chem. Soc. 2008; 130:13400–13409. [PubMed: 18781750]

(43). Speers AE, Cravatt BF. Profiling enzyme activities in vivo using click chemistry methods. Chem. Biol. 2004; 11:535–546. [PubMed: 15123248]

(44). Speers AE, Cravatt BF. Chemical strategies for activity-based proteomics. ChemBioChem. 2004; 5:41–47. [PubMed: 14695510]

(45). Kolb HC, Finn MG, Sharpless KB. Click chemistry: Diverse chemical function from a few good reactions. Angew. Chem., Int. Ed. 2001; 40:2004–2021.

(46). Lewis WG, Green LG, Grynszpan F, Radic Z, Carlier PR, Taylor P, Finn MG, Sharpless KB. Click chemistry in situ: Acetylcholinesterase as a reaction vessel for the selective assembly of a femtomolar inhibitor from an array of building blocks. Angew. Chem., Int. Ed. 2002; 41:1053–1057.

(47). Rostovtsev VV, Green LG, Fokin VV, Sharpless KB. A stepwise Huisgen cycloaddition process: Copper(I)-catalyzed regioselective “ligation” of azides and terminal alkynes. Angew. Chem., Int. Ed. 2002; 41:2596–2599.

(48). Wang Q, Chan TR, Hilgraf R, Fokin VV, Sharpless KB, Finn MG. Bioconjugation by copper(I)-catalyzed azide-alkyne [3+2] cycloaddition. J. Am. Chem. Soc. 2003; 125:3192–3193. [PubMed: 12630856]

(49). Speers AE, Cravatt BF. Activity-Based Protein Profiling (ABPP) and Click Chemistry (CC)-ABPP by MudPIT Mass Spectrometry. Curr. Protoc. Chem. Biol. 2009; 1:29–41. [PubMed: 21701697]

(50). Rawlings ND, Waller M, Barrett AJ, Bateman A. MEROPS: the database of proteolytic enzymes, their substrates and inhibitors. Nucleic Acids Res. 2014; 42:D503–D509. [PubMed: 24157837]

(51). Liu Y, Chen J, Sethi A, Li QK, Chen L, Collins B, Gillet LC, Wollscheid B, Zhang H, Aebersold R. Glycoproteomic analysis of prostate cancer tissues by SWATH mass spectrometry discovers N-acylethanolamine acid amidase and protein tyrosine kinase 7 as signatures for tumor aggressiveness. Mol Cell Proteomics. 2014; 13:1753–1768. [PubMed: 24741114]

(52). Ouairy CM, Ferraz MJ, Boot RG, Baggelaar MP, van der Stelt M, Appelman M, van der Marel GA, Florea BI, Aerts JM, Overkleeft HS. Development of an acid ceramidase activity-based probe. Chem. Comm. 2015 DOI: 10.1039/C1035CC00356C.

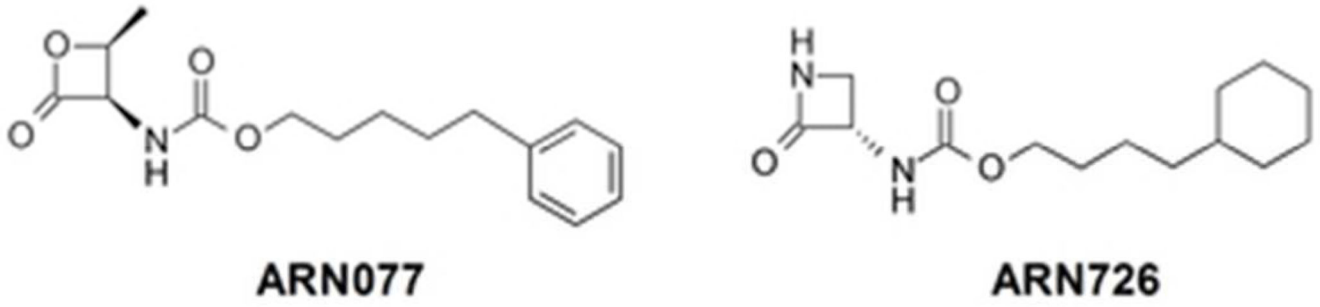

Figure 1.
Structures of NAAA inhibitors: β-lactone ARN077 and β-lactam ARN726.

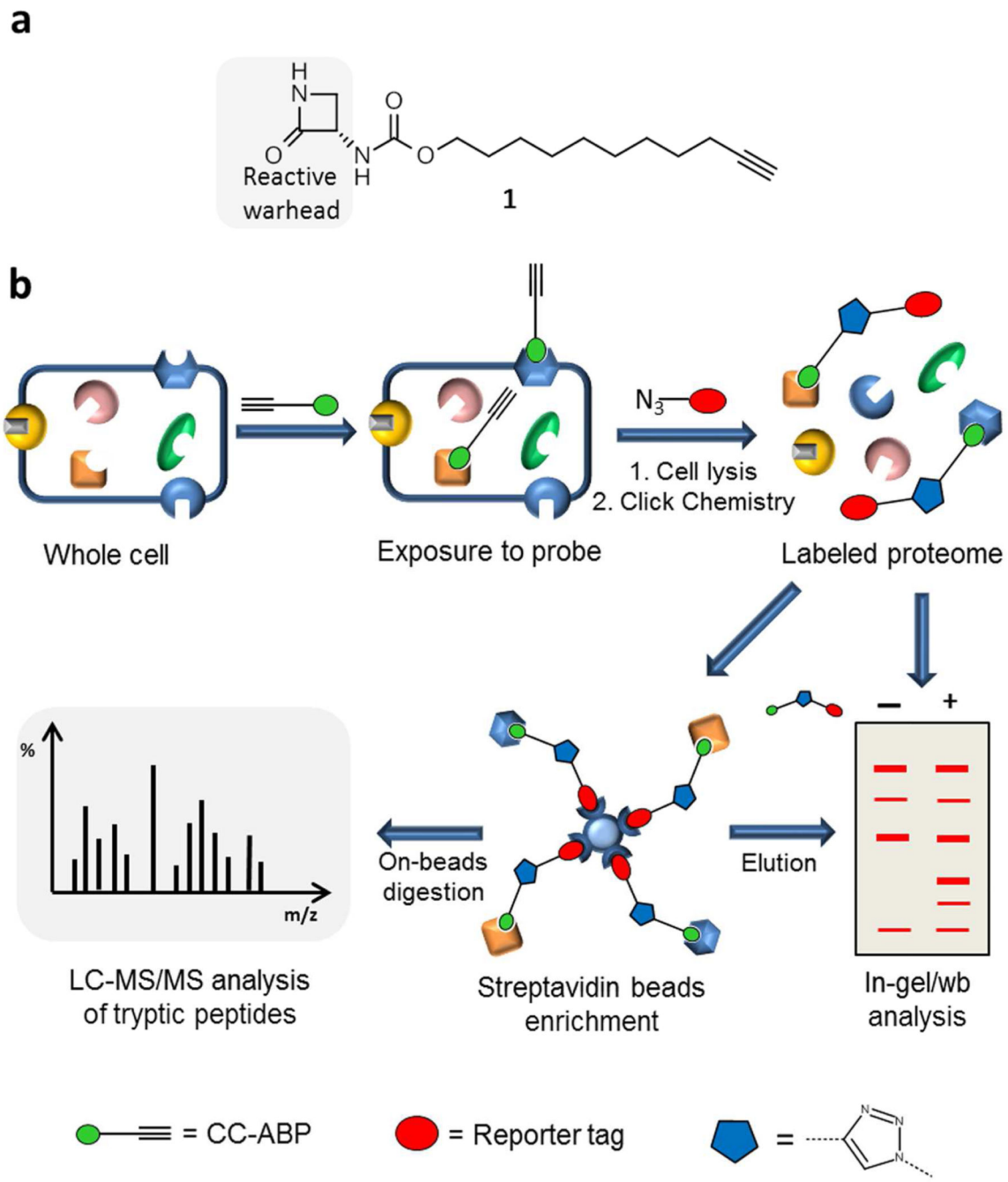

Figure 2.

(**a**) Structure of the click chemistry probe **1**. (**b**) General strategy for click chemistry activity-based protein profiling (CC-ABPP). Whole-cells or lysates are incubated with the probe and subjected to click chemistry to introduce the reporter tag. The labeled proteome is visualized by in-gel /western blot analysis before and/or after enrichment on streptavidin beads. Protein identification is carried out by mass spectrometry of the enriched proteome tryptic peptides.

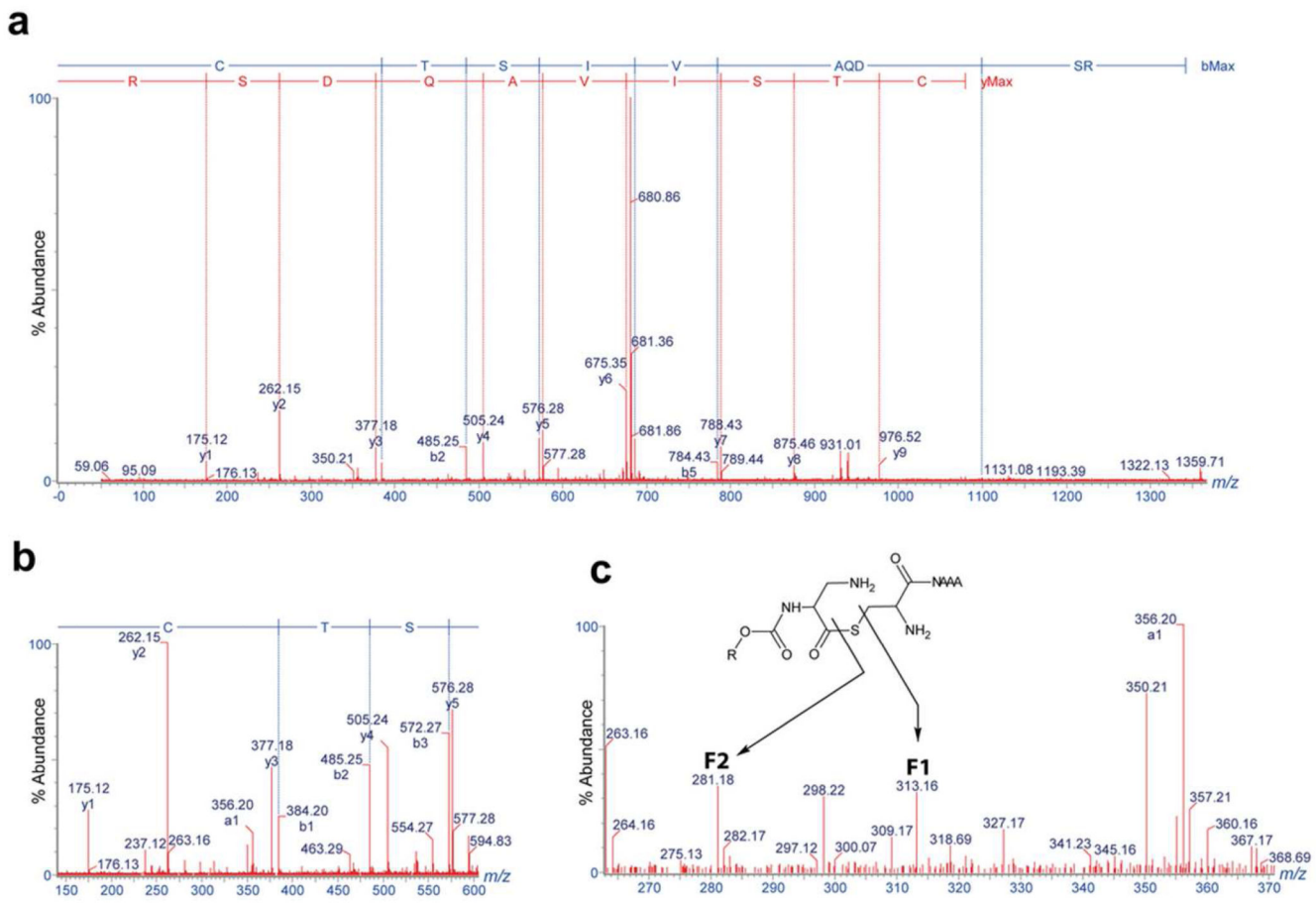

Figure 3.

(**a**): Full MS/MS spectrum of hNAAA peptide CTSIVAQGR acylated by ARN14686. (**b**): Zoomed range showing b1, b2 and b3 backbone fragment ions indicating that the acylation occurred on the N-terminal cysteine residue. (**c**): Further zoom of the same mass range, showing two side-chain fragmentations (**F1** and **F2**) that are diagnostic for a thioester formation (**F1**= $[C_{15}H_{25}N_2O_3S]^+$, expected *m/z* 313.1586, measured *m/z* 313.1580, 1.9 ppm mass error. **F2**= $[C_{15}H_{25}N_2O_3]^+$, expected *m/z* 281.1865, measured *m/z* 281.1860, 1.8 ppm mass error).

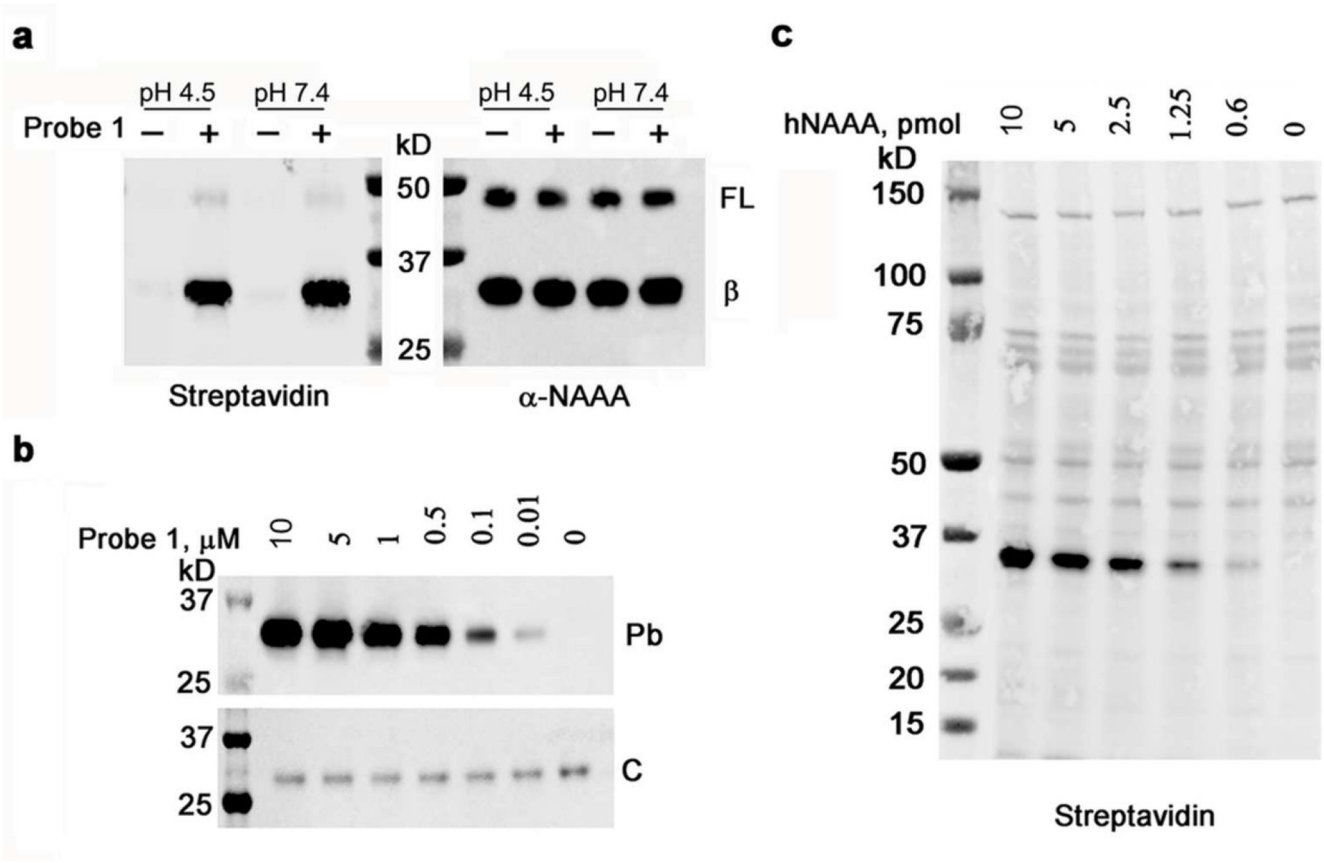

Figure 4. Labeling of purified hNAAA

(**a**) Protein blot analysis of activated recombinant hNAAA incubated with DMSO (−) or compound **1** (+) at pH 4.5 or 7.4. The blotting membranes were probed with streptavidin-HRP conjugate or anti-NAAA antibody (α-NAAA), as indicated. (**b**) Concentration dependence of the interaction of **1** with NAAA. **1** was incubated at various concentrations with a constant amount of hNAAA (1 μM). (**c**) Limit of detection of hNAAA by **1**. hNAAA was incubated at various concentrations with a constant amount of **1** (10 μM) in the presence of 10 μg of protein extract from HEK293 cells; blotting membrane in panels **a** and **c** were probed with streptavidin-HRP conjugate; FL: full-length protein; β: NAAA β–subunit; Pb = Protein blot; C = Coomassie blue staining.

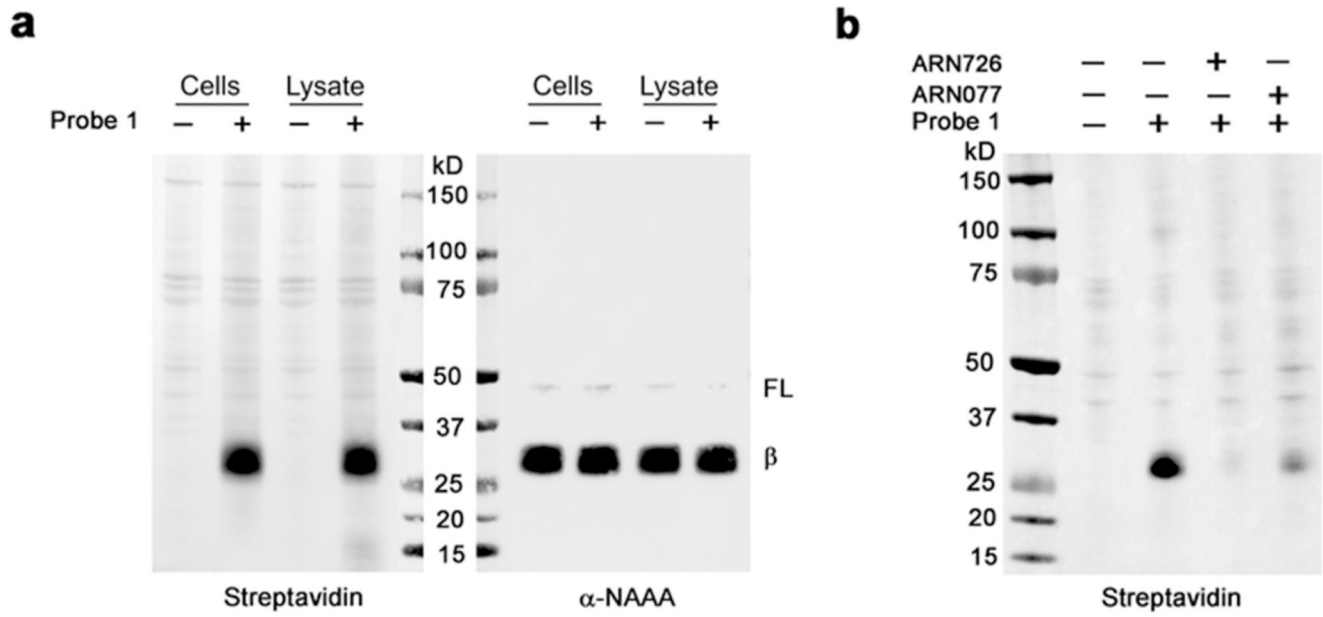

Figure 5. Labeling of hNAAA in lysed and intact NAAA-HEK293 cells

(**a**) Protein blot analysis of hNAAA-overexpressing HEK293 intact cells (lane 1 and 2) or lysate (lane 3 and 4) incubated with **1** (+) or DMSO (−). (**b**) hNAAA-HEK intact cells preincubated with ARN726 (lane 3) or ARN077 (lane 4) before addition of **1**. Cells incubated with DMSO (lane 1) or **1** only (lane 2) were used as controls. The blotting membranes were probed with a streptavidin-HRP conjugate or an anti-NAAA antibody (α-NAAA) as indicated in the figure. FL: full-length protein; β: NAAA β–subunit.

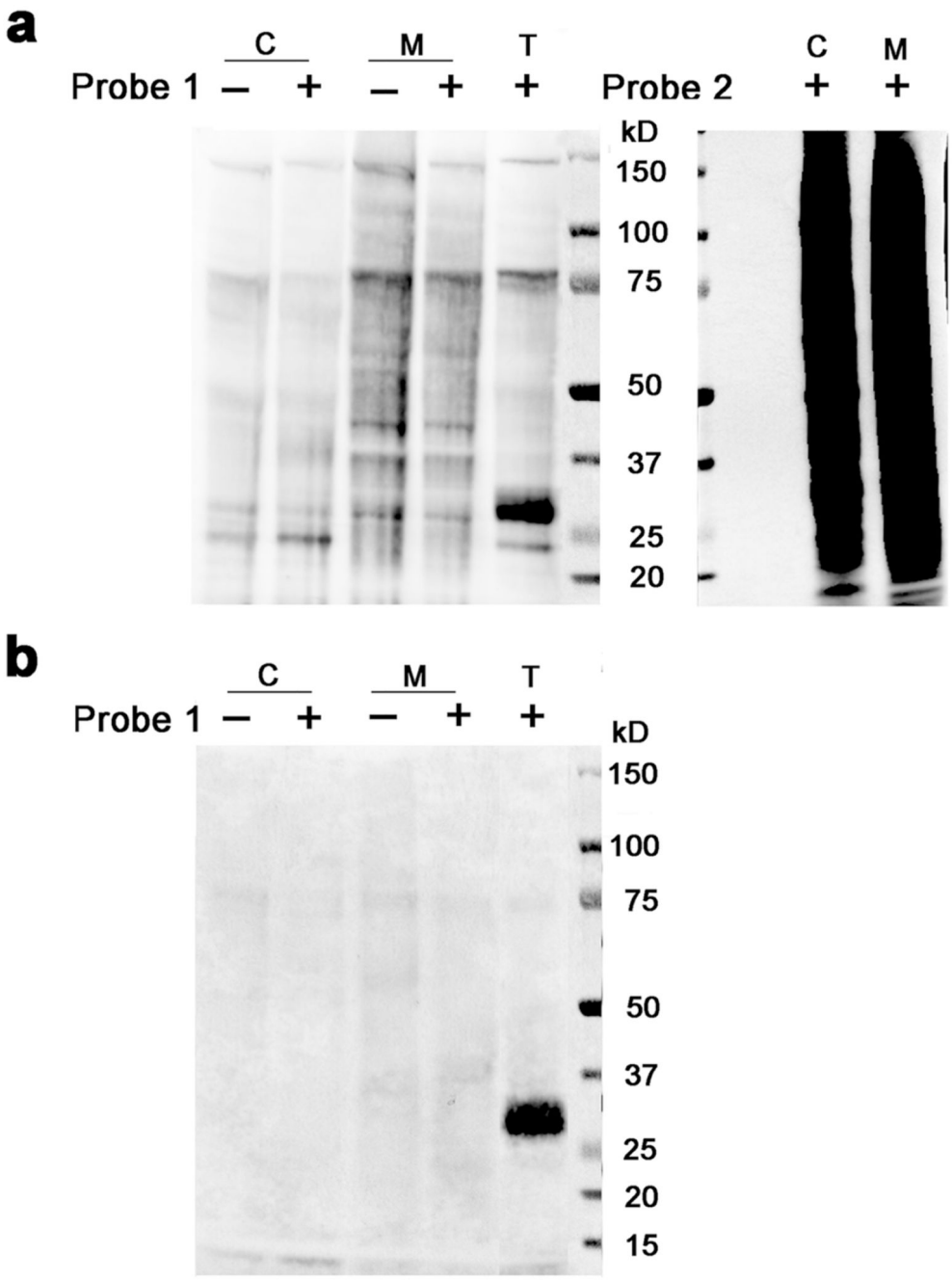

Figure 6. Probe labeling profile of wild-type HEK293 cells

(**a**) Protein blot analysis performed on cellular fractions from wt HEK293 cells incubated with **1** (left membrane) or **2** (right membrane). The total cell lysate of NAAA-HEK293 cells incubated with **1** was used as positive control (lane 5, left membrane). (**b**) Protein blot analysis of **1** incubated samples enriched on streptavidin-agarose and eluted. Blotting membranes were probed with a streptavidin-HRP conjugate. C: cytosol; M: membranes; T: total lysate

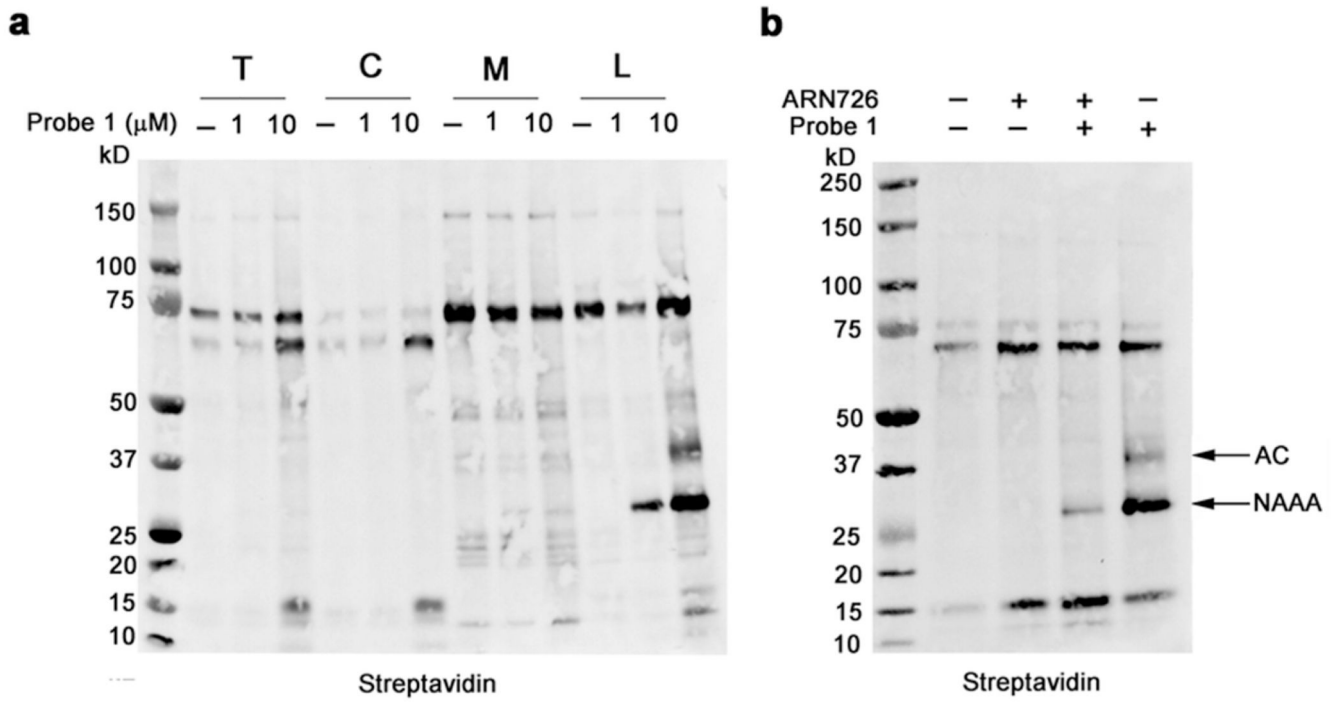

Figure 7. In vitro and in vivo probe labeling profile of rat lungs

(**a**) Protein blot analysis of streptavidin-enriched proteins from rat lung cellular fractions incubated in vitro with **1** (1 μM or 10 μM) or DMSO as negative control (−). (**b**) Protein blot analysis of streptavidin-enriched proteins of lung lysosomal fractions from rats intravenously injected with ARN726 followed by **1** (lane 3) or with **1** only (lane 4). Treatment with vehicle (lane 1) or ARN726 alone (lane 2) were used as negative controls. Blotting membranes were probed with a streptavidin-HRP conjugate. Signals corresponding to AC and NAAA are indicated. T: total lysate; M: membranes; C: cytosol; L: Lysosomes.